Original Article

Contrast Enhancement of Scintigraphic Image Using Fuzzy Intensification

Anil Kumar Pandey, Sakshi Dogra, Param Dev Sharma[1], Jasim Jaleel, Chetan Patel, Rakesh Kumar

Department of Nuclear Medicine, All India Institute of Medical Sciences, [1]Department of Computer Science, SGTB Khalsa College, University of Delhi, New Delhi, India

Abstract

Introduction: The objective of this study was to see the effect of fuzzy intensification (INT) operator on enhancement of scintigraphic image. **Materials and Methods:** Nuclear medicine physician (NMP) provided 25 scintigraphic images that required enhancement. The image pixels value was converted into fuzzy plane and was subjected to contrast INT operator with parameters of INT operator i.e., cross-over = 0.5 and number of iterations = 1 and 2. The enhanced image was again brought back into spatial domain (de-fuzzification) whose intensity value was in the range 0–255. NMP compared the enhanced image with its input image and labeled it as acceptable or unacceptable. The quality of enhanced image was also accessed objectively using four different image metrics namely: Entropy, edge content, absolute mean brightness error and saturation metrics. **Results:** Most of the enhanced images (18 out of 25 images) obtained at cross-over = 0.5 and number of iterations = 1 are acceptable and found to have overall better contrast compared to the corresponding input image. Four images (two brain positron emission tomography scan and two I-131 scan) obtained at cross-over = 0.5 and with iteration = 2 are acceptable. Three input images (one dimercaptosuccinic acid (DMSA), one I-131 and one I-131- metaiodo-benzyl-guanidine (MIBG) scan**)** were better than their enhanced images. **Conclusions:** The enhancement produced by fuzzy INT operator was encouraging. Majority of enhanced images were acceptable at cross-over = 0.5 and number iterations = 1.

Keywords: *Contrast enhancement, fuzzy intensification operator, scintigraphic image*

Introduction

We aspire to see the true distribution of radioactivity inside the body in a scan. To be able to achieve this, the image must be sharp such that activity in each compartment (tissue or organ) can be easily perceived distinctly and each compartment should look as an independent entity in the image. However, such an ideal image is far from the real ones which we observe in routine nuclear medicine practice. Various types of images are observed: Images that have very high global contrast (difference in maximum and minimum count is very high but there is lack of local contrast so that the details in entire image canvas are not visible), blurry images having boundaries of one uptake region merged with another structure in the image so that tracing the accurate boundary of an object is difficult, images with uptake differences in target object and the background (structures other than the target object in the image) is too small to be viewed clearly and label the target object representing a disease confidently, images with target object blurred and embedded in the noisy background making the detectability of small lesions ambiguous and also lowering the confidence in making decision regarding the presence of a disease, and so on. Such images require some kind of mathematical manipulation of pixel values so that the relevant details get prominence in the image and irrelevant details are suppressed.

Several image processing techniques are used to enhance images starting from simple window-level contrast enhancement tool to state of the art algorithms which sharpen the image and also remove noise while preserving edges.[1-3] In particular, several image processing techniques have been explored for enhancing the quality of scintigraphic images[4-8] Fuzzy intensification (INT) operator has been used for image enhancement in fields other than nuclear medicine but has yet not been used by nuclear medicine community for contrast enhancement of images.[9-11]

In this pilot study, we have applied the fuzzy INT operator on a set of 25 nuclear medicine images to improve their quality. The quality of the enhanced images was evaluated by nuclear medicine

How to cite this article: Pandey AK, Dogra S, Sharma PD, Jaleel J, Patel C, Kumar R. Contrast enhancement of scintigraphic image using fuzzy intensification. Indian J Nucl Med 2022;37:209-16.

Address for correspondence:
Dr. Anil Kumar Pandey, Department of Nuclear Medicine, All India Institute of Medical Sciences, Ansari Nagar, New Delhi - 110 029, India.
E-mail: akpandeyaiims@gmail.com

Received: 31-12-2021
Revised: 04-03-2022
Accepted: 16-03-2022
Published: 02-11-2022

Access this article online

Website: www.ijnm.in

DOI: 10.4103/ijnm.ijnm_210_21

Quick Response Code:

physician (NMP) for acceptability. Here, we report the results of this investigation.

Materials and Methods

The contrast INT operator on a fuzzy set A generates another fuzzy set $A' = INT(A)$ in which the fuzzification is reduced by increasing the values of $\mu_A(x_{mn})$ which are above 0.5 and decreasing those which are below it. We define this INT operator[11] by a transformation T_1 of the membership function μ_{mn} as

$$T_1(\mu_{mn}) = T'_1(\mu_{mn}) = 2\mu_{mn}^2 \quad 0 \le \mu_{mn} \le 0.5$$
$$= T''(\mu_{mn}) = 1 - 2(1 - \mu_{mn})^2 \qquad (1)$$
$$0.5 \le \mu_{mn} \le 1$$
$$m = 1,2,\ldots M, n = 1,2,\ldots.$$

In general, each μ_{mn} modified to μ'_{mn} to enhance the image X in the property domain by a transformation function T_r where

$$\mu'_{mn} = T_r(\mu_{mn}) = T'_r(\mu_{mn}), 0 \le \mu_{mn} \le 0.5$$
$$= T''_r(\mu_{mn}), 0.5 \le \mu_{mn} \le 1$$
$$r = 1,2,\ldots$$

The transformation function T_r is defined as successive applications of T_1 by the recursive relationship

$$T_s(\mu_{mn}) = T_1\{T_{S-1}(\mu_{mn})\}, s = 1,2,\ldots$$

And $T_1(P_{mn})$ represents the operator INT defined in eq. (1)

As r increases, the enhancement function in $\mu_{mn} - \mu'_{mn}$ plane tends to be stepper because of the successive application of INT. In the limiting case, as $r \to \infty$, T_r produces a two level (binary) image. It is to be noted here that, corresponding to a particular operation of T', one can use any of the multiple operation of T" and vice-versa to attain a desired amount of enhancement. Similarly, some other enhancement functions can be used independently instead of these used in equation (1).

The membership plane μ_{mn} for enhancing contrast around a cross over point may be obtained from

$$\mu_{mn} = G(x_{mn}) = \left[1 + \left(|\hat{x} - x_{mn}| / F_d\right)^{Fe}\right]^{-1}$$

Where the position of crossover points bandwidth and hence the symmetry of the curve are determined by the fuzzifiers F_e and F_d. when $\hat{x} = x_{mn}$ (maximum level in X), μ_{mn} represents an S-type function. When $\hat{x}$ = any arbitrary level l, μ_{mn} represent a π-type function.

After enhancement in fuzzy property domain, x'_{mn} the enhanced spatial domain may be obtained from

$$x'_{mn} = G^{-1}(\mu'_{mn}), \alpha \le \mu'_{mn} \le 1$$

Where α is the μ_{mn} value of when $x_{mn}=0$

The essence of above mathematical description of fuzzy INT operator and how this operator is helpful in improving the contrast of a given image can be explained graphically. Figure 1 illustrates the nature of INT operator. The illustration is based on the assumption that input image has pixel counts ranging from 0 to 255 (which is shown as input image pixel counts on X-axis), and after application fuzzy INT operator the pixel counts ranges from 0 to 1 as output image pixel counts on Y-axis. For a cut-off value = 0.5, using equation (1) three different curves have been generated at number of iterations 1, 2, and 4.

The transition of pixel counts above and below the cut-off value = 0.5, (corresponds to 128 input image pixel counts) is symmetrical, the bright pixels (greater pixel counts) become brighter and dark pixels (smaller pixel counts) become darker. Thus, the nature of the operator to make bright pixel brighter and dark pixel darker creates the contrast in the image.

It is to be noted that with the increase in the number of iterations, slope of the curve becomes steeper (meaning that operator is going to create relatively increased contrast with increase in number of iterations, a time will come when the contrast will become maximum (i.e., the image will become a binary image having only two values: 0 and 1.). On visual inspection, it can be confirmed that the curve corresponding to number of iterations = 1 have lowest slope and curve corresponding to number of iterations = 4 has highest slope. Thus, the enhanced image obtained with number of iterations = 4 will have maximum contrast and the enhanced image obtained with number of iterations = 1 will have minimum contrast.

In this pilot study, the motivation for selecting the cutoff value as 0.5 is based on the article published by Pal and King,[11] in which they have demonstrated very good performance of fuzzy INT operator at this cutoff value.

Images in data set

The pilot study included 25 scintigraphic images two F-18 fluorodeoxyglucose (F-18-FDG) brain scan images, nine F-18-FDG liver scan images, three Tc-99 m

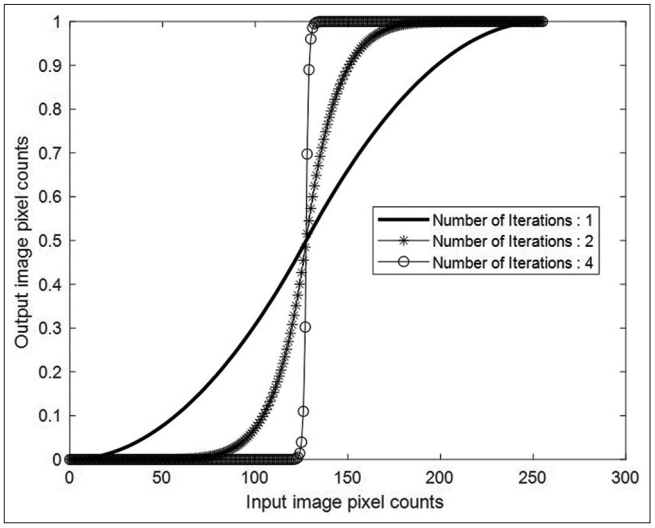

Figure 1: Illustrating nature of fuzzy intensification operator

dimercaptosuccinic acid (Tc-99 m DMSA) renal scan images, three Tc-99 m methylene diphosphonate (Tc-99 m MDP) bone scan images, one Tc-99 m pertechnetate thyroid scan images, one Tc-99 m sestamibi parathyroid scan images, and six I-131 metaiodobenzylguanidine (I-131 mIBG) scan images, [Figure 2] acquired between April 2021 and July 2021 during of routine investigation at our facility. The acquisition protocols used for these images are as follows:

F-18-FDG positron emission tomography (PET) scan images (two brain and nine liver scan images) were acquired on integrated PET-computed tomography (CT) system (Biograph mCT, Siemens Medical Solutions, Erlangen, Germany). Patients had glucose level ≤7.7 mmol/l and had fasted for at 4 h underwent PET/CT scan 45–60 min after intravenous injection of 370 MBq of F-18-FDG.

Images acquired with covering the patient from skull apex to midthigh in the liver and in case of brain from apex of the skull to the base of the skull. PET bed size matched the CT FOV. PET acquisition was performed just after CT on covering the same field of view. The acquisition time per bed position for the liver and brain study was 2 min and 15 min, respectively.

The acquired images in 128 × 128 matrix were reconstructed using the order subset expectation maximization algorithm with 2 iterations and 8 subsets, and full width half maximum of 5 mm. CT-based attenuation correction of the PET images was applied. The attenuation corrected PET images have been included in the study.

Planar gamma camera images **(**three Tc-99 m-DMSA renal scan images, three Tc-99 m-MDP-bone scan images, one Tc-99 m-pertechnetate thyroid scan images, one Tc-99 m-MIBI-parathyroid scam image, six I-131-mIBG scans images**):** Tc-99 m-DMSA-renal scan was performed after 4–6 h of administration of radiopharmaceuticals on Siemens Symbia E Dual Head Gamma camera (Siemens Medical Solutions, Illinois, USA) equipped with low energy high resolution (LEHR) collimator Posterior, Right Posterior oblique and Left Posterior oblique views were acquired with a zoom 1.45 for 250 KiloCounts in 256 × 256 matrix. Whole body Tc-99 m-MDP bone scan image was performed on Symbia T6 single-photon emission computed tomography/CT (SPECT/CT) scanner (Siemens Medical Solutions, Illinois, USA) equipped with LEHR collimator. The scan speed was 20 cm/min and images were acquired

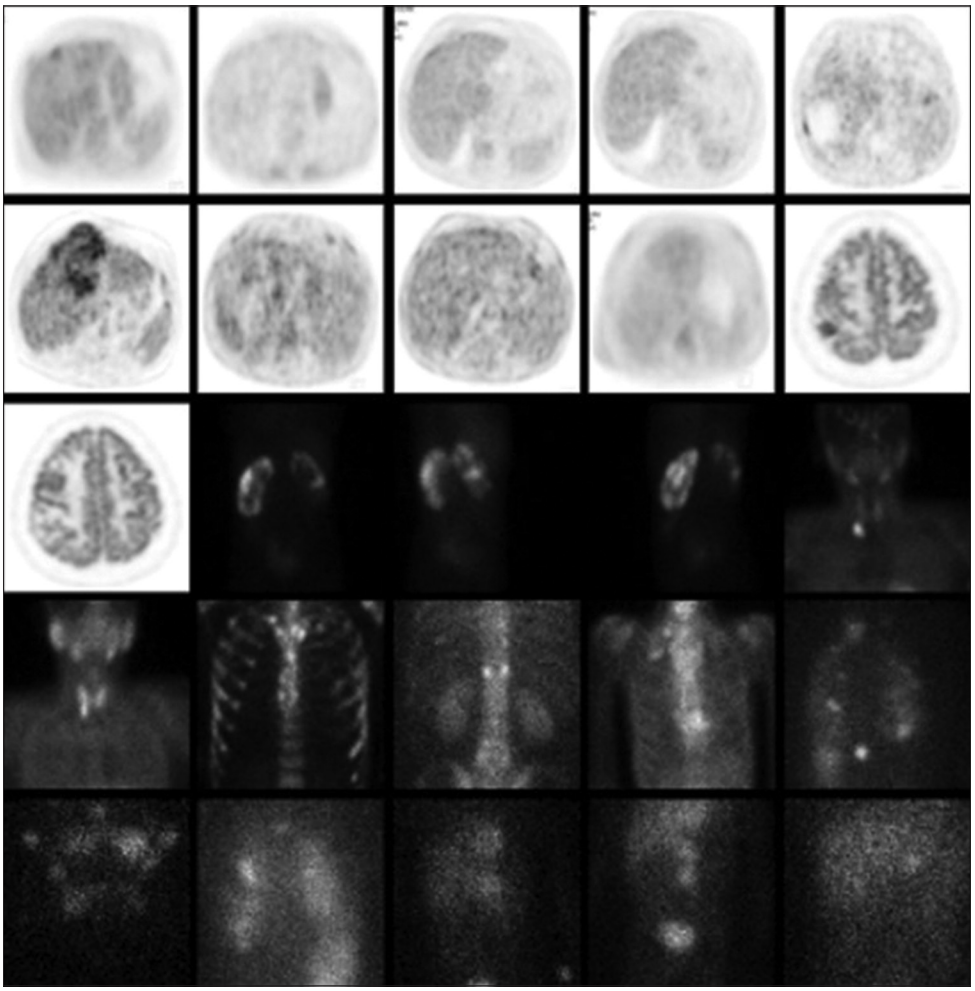

Figure 2: All 25 images include in the study

in 1024 × 256 matrix. I-131-mIBG scan was performed on high energy collimator with the speed of 10 cm/min in continuous mode with 1024 × 256 matrix size on GE Discovery 670 NM/CT (General Electrical Healthcare, Illinois, USA).

Tc-99 m-MIBI parathyroid scan images were acquired using the following acquisition protocol: 15–20 mci-MIBI was administered intravenously to the patient, and planar images were acquired at 15 min, 50 min and 2-hr after the radiopharmaceutical administration on Siemens Symbia T6 Dual Head Gamma camera and SPECT/CT (Siemens Medical Solutions, Illinois, USA) equipped with LEHR collimator at zoom 2.0 and 700 Kilo counts. The images included in this study were the images acquired at 2-h.

The image enhancement using fuzzy INT operator involved the following steps: (1) read the image, (2) fuzzify the image data (all pixel values after fuzzification should be in the range 0–1), (3) modify the pixel values for contrast INT: If the pixel value is ≤0.5, then enhanced pixel value = 2 × (pixel value)^2 else enhanced pixel value = 1–2 × (1-pixel value)^2. Iterate this step for required number of iterations, (4) defuzzify (bring all the pixel values between 0 and 255), and (5) save the enhanced image.

Subjective assessment of image quality

Images were placed on PowerPoint slides. On each slide, there were three images: Input image, enhanced image at iteration 1 and enhanced image at iteration 2 [A representative slide is shown in Figure 3]. Enhanced images were categorized into two groups: Acceptable or unacceptable.

The enhanced image [Figure 3c and f] having any of the characteristics: (Outline/contour of the object, loss of object/structure, over enhancement), were categorized as unacceptable.

Objective assessment of image quality

Second order entropy (*Entropy*),[12] edge-based contrast metric (EBCM),[13] absolute mean brightness error (AMBE),[14] and saturation evaluation metrics (SEM)[15] were used for objective assessment of the contrast in the image. A good quality image has (i) low AMBE, (ii) low SEM, (iii) well preserved edges (i.e., change in EBCM should be zero), and (iv) decrease in entropy as a result of image enhancement algorithm. The formulas used for calculation of entropy, EBCM, AMBE, and SEM are given in Table 1.

Statistical analysis

Test of normality (Shapiro–Wilk's test) was applied on the image quality metrics data. Those data sets which passed the test of normality were subjected for paired *t*-test. Paired *t*-test was conducted to determine whether the means of the two groups (image quality metrics [AMBE, EBCM, SEM, and Entropy] at iteration = 1 and iteration = 2) are equal to each other. The null hypothesis was that the two means are equal at. Those datasets that failed to pass the test of normality were subjected to *Wilcoxon signed-rank* test with continuity correction. We used open-source software R for

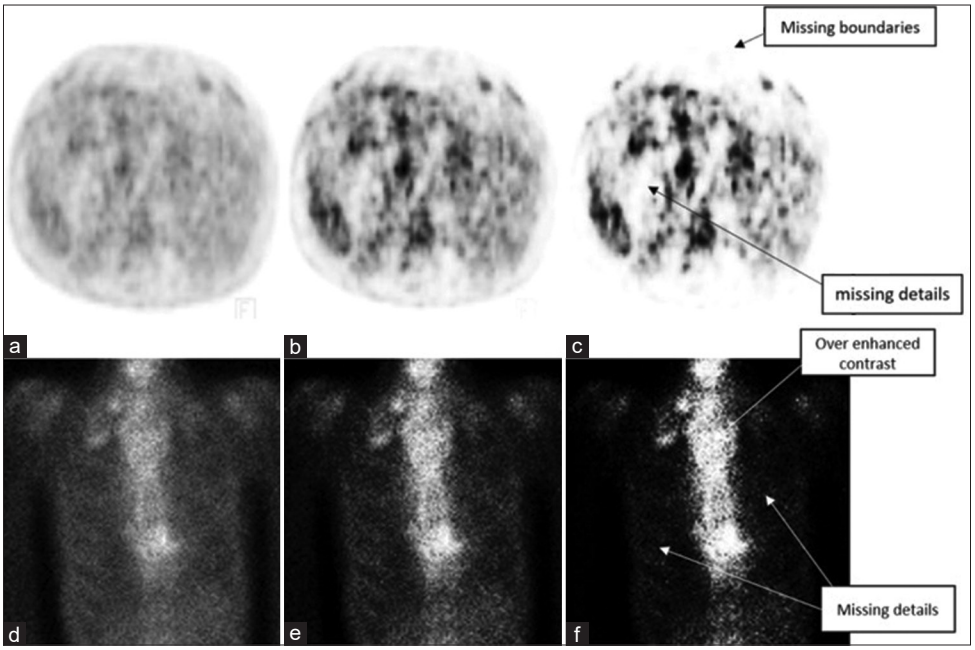

Figure 3: (a), Input image. (b), input image a after iteration 1. (c), input image a after iteration 2. (d), input image. (e), input image d after iteration 1. (f), input image d after iteration 2. Image (b) shows enhanced contrast, no loss of boundaries and details. Image (c) shows enhanced contrast but the boundaries missing and some details also missing. In image (e) no over enhancement of contrast and no missing details. In image (f), over enhanced contrast and details are also missing

statistical analysis (R Core team, R foundation for stastical computing, Vienna, Austria).[16]

Results

The overall contrast in the enhanced image (obtained after 1st iteration) was found to be better than its corresponding input image. Figure 3 shows a sample case of input and enhanced images (2a and 2d are input and 2b and 2e are their respective enhanced images). The global contrast was found to be better in enhanced image as compared to the corresponding input image. Further, at number of iterations = 2, the global contrast was better than that of the enhanced image obtained at iteration = 1. The radiopharmaceutical uptake became more prominent in enhanced images obtained either at iteration = 1 or iteration = 2, and signal to noise ratio is much better in the enhanced image at iteration = 2. However, at iteration = 2, loss of information was also observed because of saturation of pixels [Figure 3c and f].

Eighteen out of 25 images obtained with number of iterations = 1 were found to be acceptable to NMP [Figure 4a-i, Input images: Figure 4a, d and g, corresponding enhanced image at iteration = 1: Figure 4b, e and h].

Four images (two I-131-mIBG images and two F-18-FDG brain PET scan) obtained at iteration = 2 were found to be acceptable. One each representative image of I-131 and F-18-FDG PET scan obtained at iteration = 2 that were acceptable are shown in Figure 5 (brain PET scan: Figure 5a (input image), Figure 5c (output images), I-131-mIBG scan: Figure 5d (input image), Figure 5f [output images]). Figure 5b and e are the enhanced image at iteration = 1 is shown here to visually compare the enhanced images at iteration = 1 and iteration = 2.

In three images out of 25, input images were found to have better image quality compared to its enhanced images [Figure 6a, d and g are the input images].

In case of F-18-FDG brain scan images; enhanced image [Figure 5c], has much better signal (i.e., lesion uptake) to noise (i.e., other structures) ratio compared to its input image [Figure 5a]. In case of liver scan image; overall enhancement (both local and global contrast) was noticed, and can be verified by inspecting images [Figure 3b and c], there is much better contrast in the inner structures [Figure 3c] compared to its input image [Figure 3a].

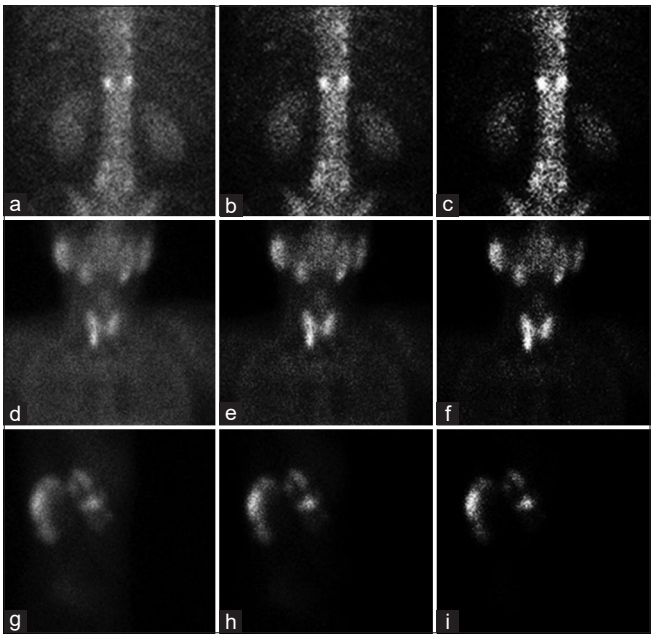

Figure 4: (a) Input image. (b) input image a after iteration 1. (c) input image a after iteration 2. (d) input image. (e) input image d after iteration 1, (f) input image d after iteration 2. (g) input image, (h) input image g after iteration 1 (i) input image g after iteration 2

Table 1: The formulas used for calculating entropy, edge-based contrast metric, absolute mean brightness error, saturation evaluation metrics

Quantity	Formula
Entropy	$\sum_{i=1}^{k}\sum_{j=1}^{k} Pij\ log_2 Pij$
	Probability P_{ij} is the *ij* th element of *G/n* where n is equal to the sum of the elements of G (G is the co-occurrence matrix)
EBCM	$\frac{1}{(m \times n)}\sum_{x_2}\sum_{x_1}\left\|\nabla c\left(\rightarrow_x\right)\right\|$
	Where m and n represent the size of the image block for which we calculate EC
	And $1 \le x_1 \le m$ and $1 \le x_2 \le n$
AMBE	$E(X) - E(Y)\ \begin{Bmatrix} X : input\ image \\ Y : Output\ image \end{Bmatrix}$
SEM	n_s=number of pixel saturated
	Where dim (x), dim (y) denotes respectively the width at the height of the image

AMBE: Absolute mean brightness error, EBCM: Edge-based contrast metric, SEM: Saturation evaluation metrics, EC: Edge content

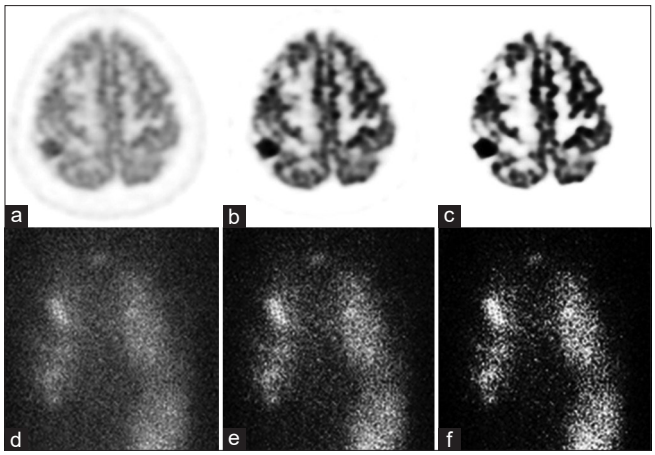

Figure 5: (a) Input image. (b) input image a after iteration 1. (c) input image a after iteration 2.(d) input image. (e) input image d after iteration 1. (f) input image d after iteration 2

In case of F-18-FDG liver scan images, the metabolic uptake is clearly visualized at both iteration 1 and 2, however, at iteration 2 the contrast is so enhanced that the enhanced image had missing boundaries and missing details which may be important while making diagnosis [Figure 3a: Input image, b: Enhanced image at iteration = 1 and c: Enhanced at iteration = 2].

Tc-99 m-MDP bone scan image and Tc-99 m-MIBI-parathyroid scan images show better uptake at iteration = 1 [Figure 4a and d] and at iteration = 2 the uptake is much more clearly visible but the body outline is missing [Figure 4c and f]. Similar types of results were also observed in case of Tc-99 m-DMSA images [Figure 4g-i].

The mean *AMBE* value (13.97) of the enhanced images at iteration = 1 were smaller than that of mean *AMBE* value (20.53) of enhanced images at iteration = 2. The result of paired *t*-test indicates that there was statistically significant difference between the means of two groups (t = −4.55, df = 24, P < 0.0001, (95% confidence interval [CI]: −9.53–3.58), mean of the differences = −6.56).

The median *EBCM* value (28.632) of the enhanced images at iteration = 1 was smaller than that of median *EBCM* value (28.632) of the enhanced images at iteration = 2. The result of Wilcoxon signed rank test with continuity correction indicates that there was insignificant difference between the median of two groups the P value which is significantly less then (V = 27, df = 24, P = 0.234).

The mean Entropy value (7.44) of the enhanced images at iteration = 1 was greater than that of mean Entropy value (5.49) of enhanced images at iteration = 2. The result of paired *t*-test indicates that there was statistically significant difference between the means of two groups (t = 11.38, df = 24, P = 3.72e-11, 95% CI: 1.59, 2.29 mean of the differences = 1.94).

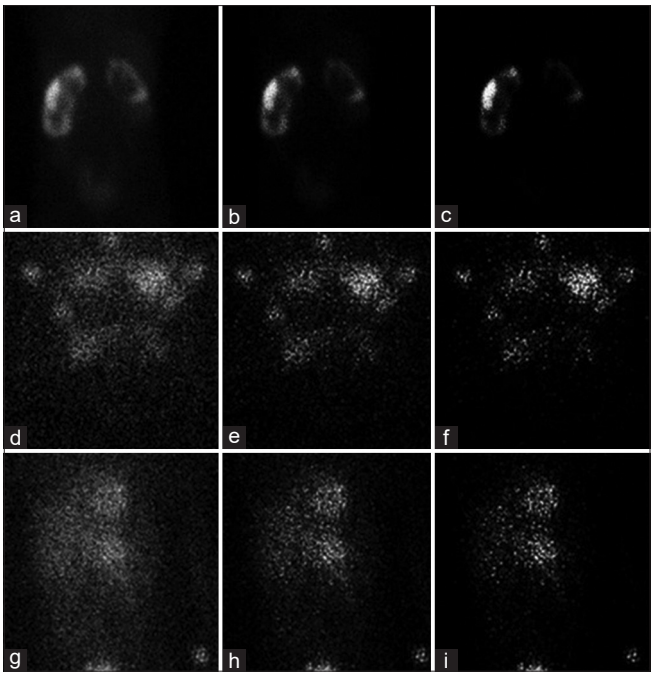

Figure 6: (a) Input image. (b) input image a after iteration 1. (c) input image a after iteration 2. (d) input image. (e) input image d after iteration 1, (f) input image d after iteration 2. (g) input image, (h) input image g after iteration 1 (i) input image g after iteration 2

The median SEM value (0.57) of the enhanced images at iteration = 1 was greater than that of median SEM value (0.52) of enhanced images at iteration = 2. The result of Wilcoxon signed rank test with continuity correction indicates that there was statistically significant difference between the median of two groups (V = 76, P = 0.004). The results of objective evaluation of the image quality agree with the result of visual assessment. The value of image quality metrics of all images in the data set is given in Table 2.

Discussion

In this plot study, we evaluated fuzzy INT operator for contrast enhancement of scintigraphic images. The experiment was conducted on a set of 25 scintigraphic images and on visual assessment we found that application of fuzzy INT operator (at number of iterations = 1) resulted in sharp image, with 18 out of 25 images generating acceptable or better image than that of the corresponding input images. Four images obtained at number of iterations = 2 was improved, while three input images were having much better contrast than their corresponding processed images The randomization of display of images or blinding the expert reading these images will influence the result. However, this has not been included in this pilot study, keeping in view the scarcity of time available from NMPs.

Due to the inclusion of penetration and scatter photons in the photo-peak energy window, in order to increase the number of counts per pixel in the limited duration of

Table 2: Result of objective assessment of image quality for both the iterations (iteration-1, iteration-2) on the basis of absolute mean brightness error, edge-based contrast metric, entropy, saturation evaluation metrics

AMBE		EBCM		Entropy		SEM	
Iteration 1	Iteration 2	Iteration 1	Iteration 2	Iteration 1	Iteration 2	Iteration 1	Iteration 2
4.89	5.30	−20.35	−20.31	−0.01	−1.60	0.31	0.18
20.46	10.05	−31.39	−31.44	1.61	0.13	0.43	0.23
9.48	21.15	−0.39	−0.4	−0.66	−3.43	0.03	0.006
10.07	20.89	−0.08	−0.08	−0.82	−3.68	0.01	0.001
3.09	8.64	−10.15	−10.32	0.38	−1.70	0.25	0.07
8.65	15.83	−2.45	−2.55	−1.29	−3.35	0.08	0.07
3.62	8.96	−25.72	−25.71	0.47	−0.71	0.32	0.14
13.59	2.95	−43.64	−43.86	1.02	0.40	0.47	0.26
4.35	19.40	−1.86	−1.77	−0.07	−1.95	0.18	0.02
7.30	9.39	0	0	−1.83	−4.65	0.63	0.63
8.48	11.63	0	0	−1.01	−3.78	0.57	0.57
6.59	8.51	0	0	−1.60	−4.32	0.57	0.57
17.77	25.40	0	0	−0.89	−3.95	0.81	0.81
20.03	34.06	0	0	−0.33	−1.46	0.82	0.82
18.70	26.81	0	0	−1.75	−5.30	0.97	0.97
23.14	38.69	0	0	−0.03	−1.09	0.93	0.93
19.61	32.90	0	0	−0.19	−1.63	0.89	0.89
22.63	33.76	0	0	−0.62	−3.59	0.99	0.99
14.03	20.57	0	0	0	−1.19	0.65	0.65
21.28	37.14	0	0	−0.001	−0.79	0.89	0.91
17.08	25.04	0	0	0	−2.50	0.85	0.85
17.67	26.16	0	0	−0.27	−2.84	0.91	0.91
21.80	35.73	0	0	0	−0.76	0.90	0.90
10.35	8.38	−42.6	−42.6	−1.57	−2.87	0.28	0.21
24.54	25.84	−66.03	−66.03	−1.19	−2.61	0.36	0.29

Negative value of entropy means image has less disorder i.e., more enhanced. AMBE: Absolute mean brightness error, EBCM: Edge-based contrast metric, SEM: Saturation evaluation metrics

imaging, the observed images had low contrast and had appreciable noise. At times in the midst of the appreciable noise, the small important clinical details fall in a zone where the clinical confidence is low to about the presence of a disease [Figure 5a]. In such cases, we expected that the fuzzy INT operator could be useful for diagnosis [Figure 5c shows improvement in F-18-FDG brain scan image].

There were three input images in which fuzzy INT operator did not perform well as NMP preferred input images compared to its enhanced images [Figure 6]. The explanation for this might be the characteristic of input image itself. Visually we can observe that the information density (counts per square cm) in these input images is very low. If comparatively large number of pixels have very small value (nearly zero), then total counts/total number of pixels in the image or in a given area of the image is low. As the image (each pixel value in the range (0–255) in spatial domain is transformed into the fuzzy plane the pixel counts are in the range (0–1) with the cross-over point at 0.5. The application of fuzzy INT operator improves the contrast by widening the gap between the minimum and maximum value by increasing the pixel value (squaring the pixel value) above the cross-over point and decreasing the pixel value (by squaring the pixel value) below the cross-over point.

This study is unique in the sense that all experiments related to the study has been performed on personal computer, with the image dataset used in the study transferred from the costly nuclear medicine processing work stations provided by the vendor. This study will inspire the young researchers to carry out the research on their personal computers, using free open-source software (such as *R*, or *Scilab*), or economy versions of proprietary software (such as MATLAB), which are rather affordable.

In this study we, investigated the fuzzy INT operator proposed by Pal and King[11] cross over value 0.5 at two iterations. At iteration number = 1, the images have adequate contrast enhancement, and iteration number = 2 there was contrast enhancement as well as some loss of details. The contrast of images was found to be enhanced by both visual (by NM physician) and objective assessment (Entropy,[12] EBCM,[13] AMBE,[14] and SEM[15]). We applied statistical analysis on objective measures of enhancement (Shapiro–Wilk's test for normality). Data set which passed the test of normality were subjected to paired *t*-test to determine whether the means of two groups are equal to each other. Datasets which failed to

pass the test of normality were subjected to Wilcoxon signed rank test.

On fuzzy image enhancement various studies have been performed.[17-22] Yet, there are very few studies done on use of fuzzy logic in nuclear medicine.[10] Pandey *et al*. have explored the utility of two fuzzy filters (triangular fuzzy filter with the moving average (TMAV) and asymmetrical triangular fuzzy filter with the moving average (ATMAV) for reducing noise from Tc-99 m sestamibi parathyroid images.[10] They investigated the effect of window size small window width (n = 3) for small level of noise, and large window (n = 5) for width for the large level of noise. There are other works on fuzzy logic in contrast enhancement that have shown have good results.[22]

Conclusions

The enhancement produced by fuzzy INT operator was encouraging. Majority of enhanced images were acceptable at cross-over = 0.5 and number iterations = 1.

Financial support and sponsorship

Nil.

Conflicts of interest

There are no conflicts of interest.

References

1. Robinson JW, Ryan JT, McEntee MF, Lewis SJ, Evanoff MG, Rainford LA, *et al.* Grey-scale inversion improves detection of lung nodules. Br J Radiol 2013;86:27961545.
2. Buades A, Coll B, Morel J. A nonlocal algorithm for image denoising. In: 2005 IEEE Computer Society Conference on Computer Vision and Pattern Recognition (CVPR'05). San Diego, CA, USA. 2005;2:605.
3. Danielyan A, Katkovnik V, Egiazarian K. BM3D frames and variational image deblurring. IEEE Trans Image Process 2012;21:1715-28.
4. Todd-Pokropek A. Medical image processing. In: Haralik RM, editor. Pictorial Data Analysis. NATO ASI Series. Vol. F4. Berlin: Springer-Verlag; 1983. p. 295-320.
5. ToddPokropek A. Image processing in nuclear medicine. IEEE Trans Nucl Sci 1980;NS27:108094.
6. Pandey AK, Sharma PD, Dheer P, Parida GK, Goyal H, Patel C, *et al.* Investigating the role of global histogram equalization technique for ^{99m}technetium-methylene diphosphonate bone scan image enhancement. Indian J Nucl Med 2017;32:283-8.
7. Pandey AK, Sharma PD, Sharma A, Negi A, Parida GK, Goyal H, *et al.* Improving technetium-99m methylene diphosphonate bone scan images using histogram specification technique. World J Nucl Med 2020;19:224-32.
8. Pandey AK, Dhiman V, Sharma A, ArunRaj ST, Baghel V, Patel C, *et al.* Role of an intensity-transformation function in enhancement of bone scintigraphy images. J Nucl Med Technol 2018;46:274-9.
9. Hanmandlu M, Jha D. An optimal fuzzy system for color image enhancement. IEEE Trans Image Process 2006;15:2956-66.
10. Pandey AK, Kumar N, Dhiman S, Patel C, Bal C, Kumar R. Fuzzy logic-based moving average filters for reducing noise from Tc-99m-sestamibi parathyroid images. Nucl Med Commun 2021;42:855-65.
11. Pal SK, King RA. Image enhancement using fuzzy set. Electron Lett 1980;16:376-8.
12. Pal NR, Pal SK. Entropic thresholding. Signal Process 1989;16:97-108.
13. Saleem A, Beghdadi A, Boashash B. Image quality metrics based multifocus image fusion. In 3rd European Workshop on Visual Information Processing. Paris, 2011; p: 77-82.
14. Chen SD, Ramli AR. Minimum mean brightness error bi-histogram equalization in contrast enhancement. IEEE Trans Consum Electron 2003;49:1310-9.
15. Hautiere N, Tarel JP, Aubert D, Dumont E. Blind contrast enhancement assessment by gradient ratioing at visible edges. Image Anal Stereol J 2008;27:87-95.
16. R Core team. A language and environment for stastical computing. R foundation for stastical computing, Vienna, Austria 2021. URL https://www.R-project.org/ [Last accessed on 2022 Apr 26].
17. Lee CS, Kuo YH, Yu PT. Weighted fuzzy mean filters for image processing. Fuzzy Sets Syst 1997;89:157-80.
18. Van De Ville D, Nachtegael M, Van der Weken D, Kerre EE, Philips W, Lemahieu I. Noise reduction by fuzzy image filtering. IEEE Trans Fuzzy Syst 2003;11:429-36.
19. Mittal P, Saini RK, Jain NK. Image enhancement using fuzzy logic techniques. In: kanad Ray, Tarun K. Sharma, Sanyog Rawat, R.K.saini, Anirban Bandyopadhyay editors. Soft Computing: Theories and Applications. Advances in Intelligent Systems and Computing. Singapore: Springer; 2019;742:537-46.
20. Kwan HK. Fuzzy filters for noise reduction in images. In: Nachtegael M, Van der Weken D, Van De Ville D, Etienne E. Kerre, editors. Fuzzy Filters for Image Processing: Springer-Verlag Berlin Heidelberg 2003;122:25-53.
21. Nachtegael M, Schulte S, Van der Weken D, De Witte V, Kerre EE. Fuzzy filters for noise reduction: The case of Gaussian noise. In: The 14th IEEE International Conference on Fuzzy Systems, 2005. FUZZ'05. Reno, Nevada, USA; 2005. p. 2016.
22. Russo F, Ramponi G. A noise smoother using cascade FIRE filters. In: Proceedings of the 4th FUZZIEEE Conference. Yokohama, Japan; 1995. p. 3518.